whereas replacements in the Tfg1 subunit of TFIIF that map to the transcription bubble shift initiation upstream[23,24]. Tfg1 is the most poorly conserved GTF between human and yeast, and it may therefore hold the key to understanding fundamental differences in start-site selection between these two transcription systems.

1. Cramer, P. *et al. Science* **288**, 640–649 (2000).
2. Cramer, P., Bushnell, D.A. & Kornberg, R.D. *Science* **292**, 1863–1876 (2001).
3. Bushnell, D.A. & Kornberg, R.D. *Proc. Natl. Acad. Sci. USA* **100**, 6969–6973 (2003).
4. Armache, K.J., Kettenberger, H. & Cramer, P. *Proc. Natl. Acad. Sci. USA* **100**, 6964–6968 (2003).
5. Gnatt, A.L., Cramer, P., Fu, J., Bushnell, D.A. & Kornberg, R.D. *Science* **292**, 1876–1882 (2001).
6. Westover, K.D., Bushnell, D.A. & Kornberg, R.D. *Science* **303**, 1014–1016 (2004).
7. Westover, K.D., Bushnell, D.A. & Kornberg, R.D. *Cell* **119**, 481–489 (2004).
8. Miller, G. & Hahn, S. A *Nat. Struct. Mol. Biol.* **13**, 603–610 (2006).
9. Hahn, S. *Nat. Struct. Mol. Biol.* **11**, 394–403 (2004).
10. Kornberg, R.D. *Trends Biochem. Sci.* **30**, 235–239 (2005).
11. Lee, D.H. *et al. Mol. Cell. Biol.* **25**, 9674–9686 (2005).
12. Lewis, B.A., Sims, R.J., III, Lane, W.S. & Reinberg, D. *Mol. Cell* **18**, 471–481 (2005).
13. Hampsey, M. *Microbiol. Mol. Biol. Rev.* **62**, 465–503 (1998).
14. Lagrange, T. *et al. Proc. Natl. Acad. Sci. USA* **93**, 10620–10625 (1996).
15. Robert, F. *et al. Mol. Cell* **2**, 341–351 (1998).
16. Forget, D., Langelier, M.F., Therien, C., Trinh, V. & Coulombe, B. *Mol. Cell. Biol.* **24**, 1122–1131 (2004).
17. Kim, T.K. *et al. Proc. Natl. Acad. Sci. USA* **94**, 12268–12273 (1997).
18. Kim, T.K., Ebright, R.H. & Reinberg, D. *Science* **288**, 1418–1422 (2000).
19. Chen, B.S., Mandal, S.S. & Hampsey, M. *Biochemistry* **43**, 12741–12749 (2004).
20. Giardina, C. & Lis, J.T. *Science* **261**, 759–762 (1993).
21. Kuehner, J.N. & Brow, D.A. *J. Biol. Chem.* **281**, 14119–14128 (2006).
22. Bushnell, D.A., Westover, K.D., Davis, R.E. & Kornberg, R.D. *Science* **303**, 983–988 (2004).
23. Ghazy, M.A., Brodie, S.A., Ammerman, M.L., Ziegler, L.M. & Ponticelli, A.S. *Mol. Cell. Biol.* **24**, 10975–10985 (2004).
24. Freire-Picos, M.A., Krishnamurthy, S., Sun, Z.W. & Hampsey, M. *Nucleic Acids Res.* **33**, 5045–5052 (2005).

Disorder breathes life into a DEAD motor

Lorraine F Cavanaugh, Arthur G Palmer III, Lila M Gierasch & John F Hunt

SecA is an essential eubacterial protein in which the ATPase motor from DEAD-box RNA helicases has adapted to function as a processive polypeptide pump. A new report suggests that a disorder-order transition in the DEAD-box motor is responsible for distinctive thermodynamic features of SecA's conformationally coupled ATPase cycle.

SecA[1] was discovered in the early 1980s as an essential factor for protein secretion in *Escherichia coli*[2]. The protein cycles between a soluble cytoplasmic form and a membrane-bound form[1,3] tightly associated with the SecYEG protein-conducting channel. Homologous channels mediate protein secretion in all organisms[4], but SecA is specific to eubacteria and chloroplasts. SecA's ATPase activity is coupled to cycles of association and dissociation with SecYEG[3] and to processive extrusion of secreted polypeptides through SecYEG[5] (that is, without back-slipping between transport steps). Although these results suggest that SecA-SecYEG association-dissociation cycles may drive polypeptide extrusion[3], the exact mechanistic relationship between these processes remains unclear.

Lorraine F. Cavanaugh and John F. Hunt are in the Department of Biological Sciences, 702A Fairchild Center, Columbia University, New York, New York 10027, USA, Arthur G. Palmer III is in the Department of Biochemistry and Molecular Biophysics, Columbia University, 630 West 168th St., New York, New York 10032, USA, and Lila M. Gierasch is in the Departments of Biochemistry & Molecular Biology and Chemistry, Lederle Graduate Research Tower 814, University of Massachusetts, Amherst, Massachusetts 01003, USA.
e-mail: jfhunt@biology.columbia.edu

Sequence analysis unexpectedly revealed that the ATPase motor in SecA is homologous to superfamily (SF)-I and SF-II ATP-dependent DNA/RNA helicases[6]. The nonprocessive SF-II 'DEAD-box' helicases most closely related to SecA unwind messenger RNA for translation[7–9], suggesting a basis for SecA's autogenous regulation of its own translation through interaction with a stem-loop in its mRNA[10]. (The name DEAD-box derives from the sequence of a characteristic extension of the Walker B ATP-binding motif.) However, other SF-I and SF-II helicases are molecular motors that processively unwind DNA and RNA helices[6,7,11], suggesting that the structural mechanics of the nucleic acid unwinding reaction may be used by SecA to drive processive polypeptide extrusion.

The ATPase motors shared by the SF-I and SF-II helicases and SecA also have structural homology to RecA[12], AAA ATPases[12], ABC transporters[13] and F1 ATPase[14,15] (**Fig. 1**), the catalytic subunit of F1F0 ATP synthetase. F1 ATPase uses mechanical work to drive ATP synthesis under aerobic conditions, but under anaerobic conditions, it runs in reverse and uses ATP hydrolysis to do mechanical work, like the SF-I and SF-II helicases and SecA. Similarity in structure and function suggests that all of these ATPases use the same fundamental structural and thermodynamic mechanisms to couple ATP hydrolysis to performance of mechanical work[12,13,16].

F1 functions as an ATP-dependent mechanical clamp, closing upon binding of ADP or ATP to an interfacial ATPase active site between tandem nucleotide-binding domains[14] (**Fig. 1a**). In contrast to F1, crystal structures of apo- and ADP-bound SecA show that the homologous DEAD-box ATPase motor in SecA has an energetic bias toward the closed ATP-bound conformation even in the absence of bound nucleotide[16] (**Figs. 1** and **2**), at least when not associated with SecYEG. However, solution studies have shown that at temperatures slightly above physiological, SecA undergoes a heat-driven, or endothermic, conformational transition (ECT) that results in drastically decreased affinity for ATP[17,18], suggesting that the clamp formed by the DEAD-box motor opens at elevated temperatures[16]. These studies support the hypothesis that the ECT in SecA reflects the ATP-dependent conformational changes that drive binding and release from SecYEG and perhaps also processive polypeptide extrusion through SecYEG.

On page 594 of this issue, Keramisanou *et al.* reveal new structural and dynamic details of the ECT in SecA[19]. They identify two polypeptide segments in the DEAD-box motor that exist in dynamic equilibrium between ordered and disordered states at physiological temperatures. Inspired by the DEAD-box helicase homology, stable constructs were produced representing most of the individual domains in SecA[20], including constructs containing either one or both of the F1-like domains comprising the DEAD-box motor. Keramisanou *et al.* use these constructs to

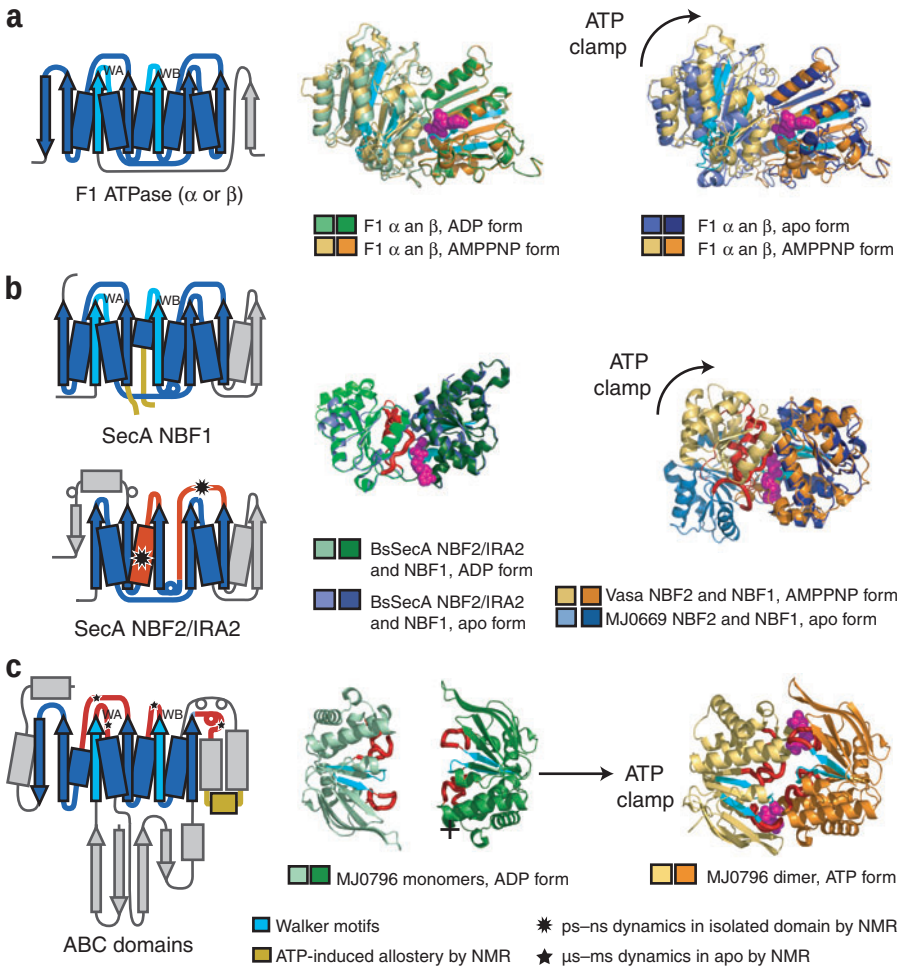

Figure 1 Structure and mechanochemistry of F1-like mechanical ATPases. Left, topology diagrams for the central ATP-binding β-sheets; right, nucleotide-bound crystal structures. NMR studies demonstrate that protein segments (red) in the ATPase active sites are dynamic in the absence of nucleotide, undergoing motions on the ps–to–ns (asterisks) or μs–to–ms timescales (small stars). ATP-binding Walker A motif (WA) and preceding β-strand and Walker B motif (WB) are highlighted in cyan; bound nucleotides are magenta. Structures are aligned on the basis of least-squares superposition of the α subunit of NBF1. (**a**) The ATPase active site in F1 ATPase[14] (PDB entry 1BMF) is formed by the Walker motifs in the β subunit at its interface with the homologous α subunit (whose Walker motifs are catalytically inactive). (**b**) The tandem F1-like motor domains in SecA are called nucleotide binding folds 1 and 2 (NBF1 and NBF2)[16]. NBF2 is also called IRA2 (refs. 19,20). The Walker motifs in NBF2/IRA2 diverge from consensus and are not known to bind ATP. Apo- (PDB entry 1M6N) and ADP-bound (1M74) *Bacillus subtilis* SecA[16] structures are similar and resemble the closed ATP-bound conformation of the DEAD-box helicase Vasa[8] (2DB3). In contrast, the DEAD-box helicase MJ0669 (1HV8) shows an open ATPase motor conformation in the apo state, with a ~45° rotation of the second F1-like domain compared to the Vasa and SecA structures[9]. PcrA exhibits a similar interdomain rotation, but of smaller magnitude (not shown). (**c**) The F1-like motor domains in ABC transporters dimerize upon binding ATP[13]. NMR dynamics studies show that most active-site loops undergo μs–to–ms motions in the apo state[22].

develop evidence that an order-disorder transition in helicase motifs V and VI (**Fig. 2**) is an intrinsic feature of the ECT and the ATP-dependent conformational reaction cycle of SecA[19], at least in the absence of SecYEG. These are the final two of the six motifs that form the interfacial ATPase active site between the two F1-like domains constituting the ATPase motors in SF-I and SF-II helicases[7].

If the ECT drives the DEAD-box motor from a closed ATP-bound conformation to an open nonbinding conformation[16,17], then nucleotide binding must be tightly coupled to the reversal of this conformational transition. Because nucleotide binding has minimal temperature dependence, whereas the ECT has a dramatic temperature dependence, Keramisanou *et al.* used affinity measurements conducted at a series of temperatures to demonstrate that an ECT similar to that in full-length SecA occurs in a construct comprising just its DEAD-box motor[19]. The authors then compare the NMR spectral properties of a construct containing both F1-like motor domains with those of a construct containing just the second of these domains (NBF2/IRA2 in **Figs. 1** and **2**) to argue that the ECT in the DEAD-box motor involves an order-disorder transition in helicase motifs V and VI. Motif IV was previously identified as populating disordered states in intact SecA[21]. Thus, combining elegant thermodynamic and spectral analyses with a divide-and-conquer domain-parsing strategy, Keramisanou *et al.* develop a chain of experimentation and reasoning that provides insight into the structural mechanics of a complex conformational transition in a large, 200-kDa dimer[19].

An order-disorder transition explains the distinctive thermodynamic features of the ECT[17,18]. A sharp endothermic transition requires both enthalpic (ΔH) and entropic (ΔS) changes to be large and positive so that a small increase in temperature (T) can drive $\Delta G = \Delta H - T\Delta S$ from a high positive value to a low negative value. The data of Keramisanou *et al.* combined with the lack of hydrophobic interdomain interfaces in the DEAD-box ATPase motor of SecA suggest that the positive ΔS results from an increase in protein-chain entropy rather than solvent entropy[19].

NMR studies of an ABC transporter ATPase domain, which shares an F1-like ATP-binding core with SecA (**Fig. 1b**,**c**), have shown that the active site loops in these F1-like domains are also disordered in the absence of bound nucleotide, with most active site loops undergoing local motions on microsecond-to-millisecond timescales in the apo state[22] (**Fig. 1c**). Such dynamic transitions occur in the apo state of many ligand-binding sites and are believed to play an important role in balancing specificity and affinity in biochemical binding reactions. Coupling of ligand binding to immobilization of protein segments allows independent optimization of binding affinity, because increasing specificity requires expanding the number of energetically favorable intermolecular interactions, which generally increases binding affinity, whereas immobilization incurs an entropic cost that reduces binding affinity. The somewhat more extensive disorder-order transition involved in reversing the ECT of SecA probably tunes the thermodynamics of its ATP-dependent conformational reaction cycle in a similar manner, but perhaps for a different reason; physiological studies *in vivo* in *E. coli* suggest that the thermodynamic properties of the

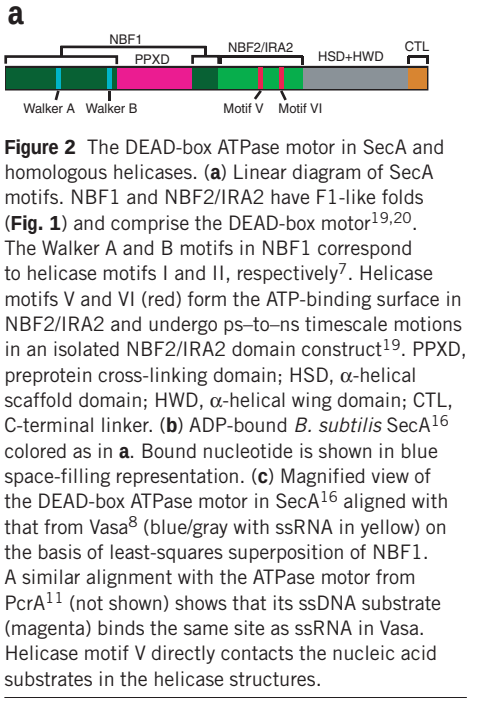

Figure 2 The DEAD-box ATPase motor in SecA and homologous helicases. (**a**) Linear diagram of SecA motifs. NBF1 and NBF2/IRA2 have F1-like folds (**Fig. 1**) and comprise the DEAD-box motor[19,20]. The Walker A and B motifs in NBF1 correspond to helicase motifs I and II, respectively[7]. Helicase motifs V and VI (red) form the ATP-binding surface in NBF2/IRA2 and undergo ps–to–ns timescale motions in an isolated NBF2/IRA2 domain construct[19]. PPXD, preprotein cross-linking domain; HSD, α-helical scaffold domain; HWD, α-helical wing domain; CTL, C-terminal linker. (**b**) ADP-bound *B. subtilis* SecA[16] colored as in **a**. Bound nucleotide is shown in blue space-filling representation. (**c**) Magnified view of the DEAD-box ATPase motor in SecA[16] aligned with that from Vasa[8] (blue/gray with ssRNA in yellow) on the basis of least-squares superposition of NBF1. A similar alignment with the ATPase motor from PcrA[11] (not shown) shows that its ssDNA substrate (magenta) binds the same site as ssRNA in Vasa. Helicase motif V directly contacts the nucleic acid substrates in the helicase structures.

ECT optimize the interaction between SecA and SecYEG for maximal transport efficiency near physiological temperature[18].

Structural studies of homologous SF-I and SF-II helicases reveal a surface groove formed in part by helicase motif V as the site where DNA or RNA helices are bound and unwound by the ATP-driven clamp-like motion of the motor domains (**Figs. 2** and **3**). Crystal structures of the SF-I helicase PcrA in complex with a single-stranded (ss) DNA substrate[11] as well as the SF-II DEAD-box helicase Vasa with an ssRNA substrate[8] (**Fig. 2c**) suggest that the ATP-driven clamp-like motion of the F1-like ATPase motor drives substrate unwinding (**Fig. 3b**,**c**). A dispensable C-terminal tail on SecA binds a site overlapping the observed DNA/RNA-binding groove in PcrA and Vasa (**Fig. 2c**) and has been proposed to occupy the functional polypeptide transport site[16]. If so, the same ATP-dependent clamp-like motion believed to drive processive DNA unwinding in PcrA (**Fig. 3c**) could drive processive polypeptide extrusion through SecYEG (**Fig. 3a**). However, given the close spatial proximity of motifs V and VI to the C-terminal tail, the order-disorder transition in these motifs characterized by Keramisanou *et al.*[19] could be precluded while a polypeptide transport substrate is bound. Thus, the dynamic transition might occur in these motifs in SecA only during cycles of binding and release from SecYEG but not during processive polypeptide extrusion through SecYEG. Alternatively, the polypeptide transport substrate might bind elsewhere in SecA rather than to this groove[23], which would imply that the mechanism of its processive extrusion differs from the mechanism of processive nucleic acid polymer unwinding by SF-I and SF-II helicases, in spite of the tantalizing hints of mechanistic similarity. Further work will be needed to resolve the similarities and differences between these intriguingly homologous systems.

1. de Keyzer, J., van der Does, C. & Driessen, A.J. *Cell. Mol. Life Sci.* **60**, 2034–2052 (2003).
2. Oliver, D.B. & Beckwith, J. *J. Bacteriol.* **150**, 686–691 (1982).
3. Economou, A. & Wickner, W. *Cell* **78**, 835–843 (1994).
4. van den Berg, B. *et al. Nature* **427**, 36–44 (2003).
5. De Keyzer, J., Van Der Does, C., Kloosterman, T.G. & Driessen, A.J. *J. Biol. Chem.* **278**, 29581–29586 (2003).
6. Koonin, E.V. & Gorbalenya, A.E. *FEBS Lett.* **298**, 6–8 (1992).
7. Cordin, O., Banroques, J., Tanner, N.K. & Linder, P. *Gene* **367**, 17–37 (2006).
8. Sengoku, T., Nureki, O., Nakamura, A., Kobayashi, S. & Yokoyama, S. *Cell* **125**, 287–300 (2006).
9. Story, R.M., Li, H. & Abelson, J.N. *Proc. Natl. Acad. Sci. USA* **98**, 1465–1470 (2001).
10. Salavati, R. & Oliver, D. *RNA* **1**, 745–753 (1995).
11. Velankar, S.S., Soultanas, P., Dillingham, M.S., Subramanya, H.S. & Wigley, D.B. *Cell* **97**, 75–84 (1999).
12. Wang, J. *J. Struct. Biol.* **148**, 259–267 (2004).
13. Smith, P.C. *et al. Mol. Cell* **10**, 139–149 (2002).
14. Abrahams, J.P., Leslie, A.G., Lutter, R. & Walker, J.E. *Nature* **370**, 621–628 (1994).
15. Kinosita, K., Jr, Adachi, K. & Itoh, H. *Annu. Rev. Biophys. Biomol. Struct.* **33**, 245–268 (2004).

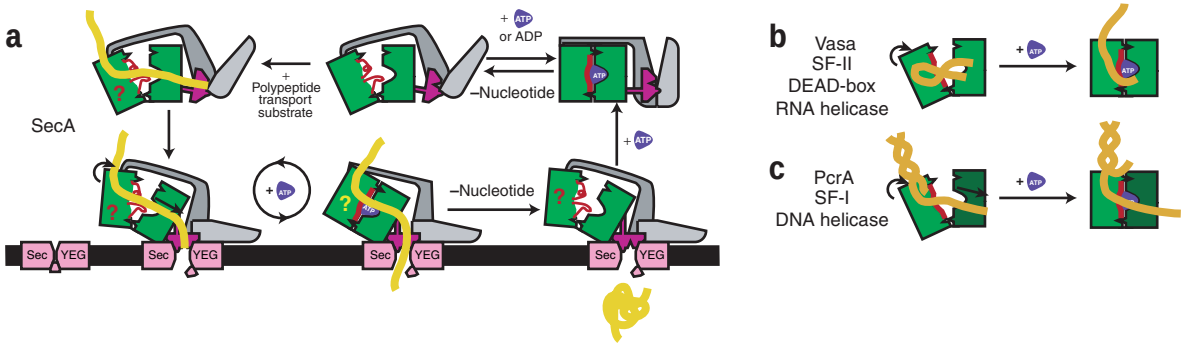

Figure 3 Possible mechanistic similarities between processive polypeptide extrusion by SecA and nucleic acid unwinding by PcrA and Vasa. ATP binding induces a clamp-like motion of the ATPase motor that could drive processive movement of polymeric transport substrates. Domains colored as in **Figure 2a**. (**a**) The polypeptide transport substrate (yellow) may displace the C-terminal linker[16] (omitted from drawing) of SecA, binding to a site spanning the interface of the two F1-like domains in the DEAD-box motor[16], analogous to the nucleic acid–binding sites in Vasa and PcrA (**b**,**c**), and extending into the preprotein cross-linking domain[23]. Helicase motifs V and VI (red) form the ATP-binding surface in the second F1-like domain. These segments probably undergo an order-disorder transition during the ECT in intact SecA free in solution[19] (upper right), though their dynamic behavior during protein translocation is unknown. (**b**) The ATP-clamp motion of the motor in Vasa unwinds an RNA stem-loop (orange) by directly pushing open the RNA helix and stabilizing ssRNA in a bent conformation incompatible with helix formation[8]. (**c**) The ATP-clamp motion of the PcrA motor unwinds a DNA double helix (orange) one base at a time, as inferred from apparent translation of the ssDNA bound to the interfacial nucleic acid–binding site[11] (PcrA-specific DNA-binding domains omitted from drawing).

16. Hunt, J.F. *et al. Science* **297**, 2018–2026 (2002).
17. den Blaauwen, T., Fekkes, P., de Wit, J.G., Kuiper, W. & Driessen, A.J. *Biochemistry* **35**, 11994–12004 (1996).
18. Ramamurthy, V., Dapic, V. & Oliver, D. *J. Bacteriol.* **180**, 6419–6423 (1998).
19. Keramisanou, D. *et al. Nat. Struct. Mol. Biol.* **13**, 594–602 (2006).
20. Sianidis, G. *et al. EMBO J.* **20**, 961–970 (2001).
21. Chou, Y.T., Swain, J.F. & Gierasch, L.M. *J. Biol. Chem.* **277**, 50985–50990 (2002).
22. Wang, C., Karpowich, N., Hunt, J.F., Rance, M. & Palmer, A.G. *J. Mol. Biol.* **342**, 525–537 (2004).
23. Papanikou, E. *et al. J. Biol. Chem.* **280**, 43209–43217 (2005).

RNA allostery glimpsed

Wade C Winkler & Charles E Dann III

Riboswitches provide an elegantly simple means of coupling metabolic sensing to genetic regulation. Recent work provides a wealth of structural insight into ligand binding by these RNAs.

RNA research has entered a renaissance during the past several years, and the degree to which genetic circuitry is tweaked at the post-transcriptional level is gradually being elucidated, suggesting that such regulation is crucial for all life. *Cis*-acting regulatory RNA elements typically interact with cellular components during stress or metabolite fluctuation. Binding of the appropriate effector induces conformational changes that alter expression of downstream genes (for examples, see **Fig. 1**). These RNAs regulate expression through control of transcription termination, translation initiation or mRNA stability (reviewed in refs. 1,2). Although some regulatory RNAs are bound by proteins or other RNAs, many directly sense small-molecule metabolites, including cofactors, amino acids, purines and even an amino sugar. Recent structural and functional data on thiamine pyrophosphate (TPP)-, *S*-adenosylmethionine (SAM)- and glucosamine-6-phosphate (GlcN6P)-sensing RNAs elegantly reveal how these RNAs build specific, high-affinity binding pockets for small, structurally diverse ligands, suggesting mechanistic models for genetic control via metabolite binding[3–6].

Historically, RNA polymers have been considered less capable of adopting specific global folds than protein counterparts, given the limited repertoire of available building blocks (4 nucleotides versus 20 amino acids) and the electrostatic problem of accommodating the polyanionic backbone. However, noncoding, structurally complex RNAs are increasingly being identified in extant organisms, and there is thus growing acceptance for the 'RNA world' theory, which suggests that RNA once accomplished all necessary catalytic and genomic roles. The intricacies of modern RNA structures are evident in the diverse classes of metabolite-sensing RNAs. The first indication of small-molecule (guanosine) recognition by RNA structures was obtained by structural resolution of the group

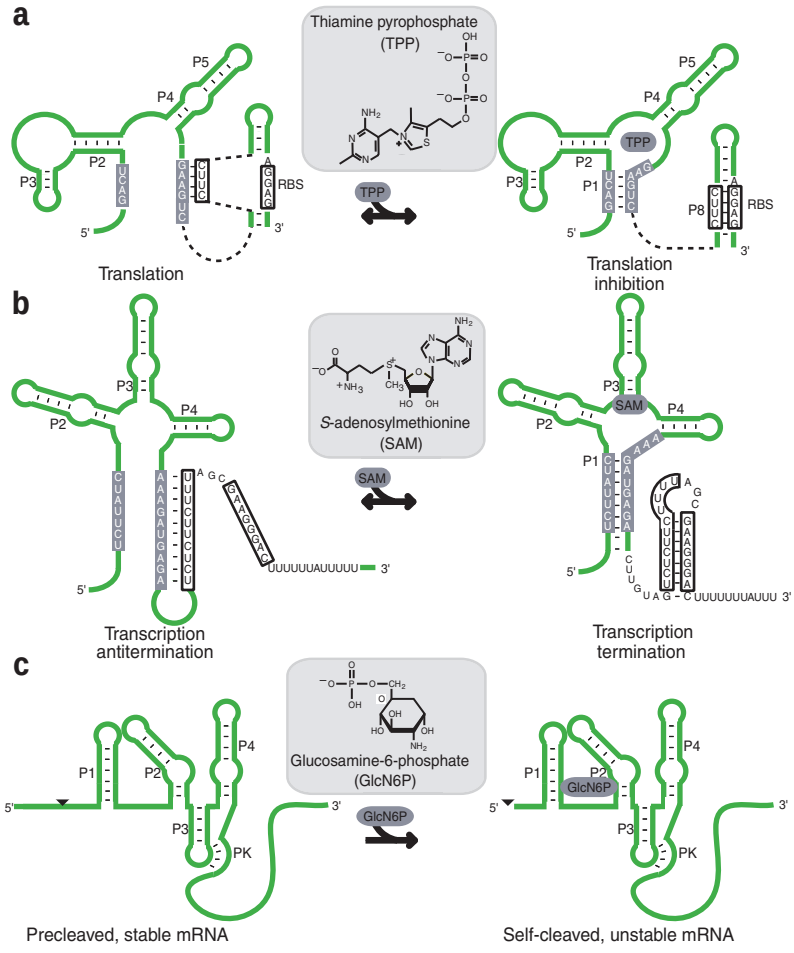

Figure 1 Genetic mechanisms of metabolite-sensing regulatory RNAs. (**a**) The *E. coli thiM* 5′ untranslated region (UTR) includes a TPP-sensing motif. TPP binds the RNA and stabilizes the P1 helix, allowing formation of a ribosome binding site (RBS)-sequestering helix. (**b**) *Thermoanaerobacter tencongensis* contains several operons putatively regulated by SAM-sensing RNAs. That used for X-ray crystallography is shown. Association of SAM stabilizes the P1 helix and promotes formation of an intrinsic transcription terminator within the 5′ UTR. (**c**) GlcN6P binds the *glmS* 5′ UTR in certain Gram-positive bacteria and stimulates an autocatalytic self-cleavage event that leads to destabilization of the overall mRNA transcript. Black triangle denotes self-cleavage site.

The authors are at the University of Texas Southwestern Medical Center, 5323 Harry Hines Blvd. Dallas, Texas 75390-9038, USA.
e-mail: wade.winkler@utsouthwestern.edu